Inorg. Chem. **2004**, *43*, 8600–8608

Luminescent Piano-Stool Complexes Incorporating 1-(4-Cyanophenyl)imidazole: Synthesis, Spectral, and Structural Studies

Sanjay K. Singh, Manoj Trivedi, M. Chandra, Abhaya N. Sahay, and Daya Shankar Pandey*

Department of Chemistry, Awadhesh Pratap Singh University, Rewa-486 003 (M.P.), India

Received June 8, 2004

Three novel luminescent piano-stool arene ruthenium complexes of general formula [(η^6-arene)$RuCl_2$(CPI)] (η^6-arene = benzene, **1**, *p*-cymene, **2**, and hexamethylbenzene, **3**; CPI=1-(4-cyanophenyl)imidazole were prepared. The molecular structures of **2** and **3** were determined crystallographically. Reaction of **1**–**3** with EPh_3 (E = P, As, or Sb) and N–N donor bases such as 2,2′-bipyridine and 1,10-phenanthroline afforded cationic mononuclear complexes of general formula [(η^6-arene)RuCl(CPI)(EPh_3)]$^+$ (η^6-arene = C_6H_6, E = P (**1a**), E = As (**1b**), E = Sb (**1c**); η^6-arene = $C_{10}H_{14}$, E = P (**2a**), E = As (**2b**), E = Sb (**2c**); η^6-arene = C_6Me_6, E = P (**3a**), E = As (**3b**), E = Sb (**3c**)) and [(η^6-arene)Ru(N–N)(CPI)]$^{2+}$ (η^6-arene = C_6H_6, N–N = bipy (**1d**), N–N = phen (**1e**); η^6-arene = $C_{10}H_{14}$, N–N = bipy (**2d**), N–N = phen (**2e**); η^6-arene = C_6Me_6, N–N = bipy (**3d**), N–N = phen (**3e**)). Molecular structures of **1a** and **2a** were also confirmed by X-ray crystallography. Structural studies of the complexes **2**, **3**, **1a**, and **2a** supported coordination of CPI through the imidazole nitrogen and the presence of a pendant nitrile group. Structural data also revealed stabilization of crystal packing in the complexes **2**, **3**, and **2a** by C–H···X (X = Cl, F) type inter- and intramolecular interactions and in complex **1a** by π–π stacking. Moreover, neutral homonuclear bimetallic complexes **2f**,**g** were prepared by using complex **2** as a metallo-ligand, where CPI acts as a bridge between two metal centers. Emission spectra of the mononuclear complexes [(η^6-arene)$RuCl_2$(CPI)] and its derivatives exhibited intense luminescence when excited in the metal to ligand charge-transfer band.

Introduction

Considerable recent attention has been paid toward designing of new homo-/hetero-binuclear complexes, in which a strong electronic interaction affords a stable mixed-valence state, because of their possible use in the study of electron-transfer reactions and in molecular scale electronic devices.[1] In search of molecular switching devices based on binuclear metal complexes, a number of systems have been developed. However, none of them have shown the ability to completely allow or block the transfer of electrons between two parts of the molecule.[2] It has been shown that certain acceptor−donor molecules exhibit twisted internal charge transfer (TICT) which appears attractive for molecular switching, since there is an almost perfect orbital decoupling in the twisted internal charge transfer state.[3] It is expected that the complexes in which redox sites are bridged by this type of molecule could be a good model to test the possibility of molecular switching. In this regard, 1-(4-cyanophenyl)-imidazole (CPI) has drawn special attention due to occurrence of twisted internal charge transfer (TICT) and the presence of two donor sites.[4] Bridging ability coupled with the twisted internal charge transfer (TICT) in CPI offers

* Author to whom correspondence should be addressed. E-mail: dsprewa@yahoo.com.

(1) (a) Willett, R. D., Gatteschi, D., Kahn, O., Eds.; *Magneto-Structural Correlations in Exchange-Coupled Systems*; Reidel: Dordrecht, Holland, 1985. (b) Meyer, T. J. *Pure Appl. Chem.* **1986**, *58*, 1193. (c) Lehn, J. M. *Supramolecular Chemistry*; VCH: Weinheim, Germany, 1995. (d) Damrauer, N. H.; Cerullo, G.; Yeh, A.; Boussie, T. R.; Shank, C. V.; McCusker, J. K. *Science* **1997**, *275*, 54. (e) Beyeler, A.; Belser, P. *Coord. Chem. Rev.* **2002**, *230*, 29.

(2) (a) Joachim, C.; Launay, J.-P. *Chem. Phys.* **1986**, *109*, 93. (b) Lehn, J.-M. *Angew. Chem., Int. Ed. Engl.* **1990**, *29*, 1304. (c) Bissell, R. A.; de Silva, A. P.; Gunaratne, H. Q. N.; Lynch, P. L. M.; Maguire, G. E. M.; Sandanayake, K. R. A. S. *Chem. Soc. Rev.* **1992**, *21*, 187. (d) Feringa, B. L.; Jager, W. F.; de Lange, B. *Tetrahedron* **1993**, *49*, 8267. (e) Gilat, S. L.; Kawai, S. H.; Lehn, J.-M. *J. Chem. Soc., Chem. Commun.* **1993**, 1439. (f) Oneil, M. P.; Niemczyk, M. P.; Svec, W. A.; Gosztola, D.; Gaines, G. L.; Wasielewski, M. R. *Science* **1992**, *257*, 63. (g) Broo, A. *Chem. Phys.* **1993**, *169*, 135. (h) Bissell, R. A.; Cordova, E.; Kaifer, A. E.; Stoddart, J. F. *Nature* **1994**, *369*, 133. (i) Rettig, W. *Angew. Chem., Int. Ed. Engl.* **1986**, *25*, 971. (j) Lippert, E.; Rettig, W.; Bonacickoutecky, V.; Heisel, F.; Miehe, J. A. *Adv. Chem. Phys.* **1987**, *68*, 1.

(3) Sowinska, M.; Launay, J.-P.; Mugnier, J.; Pouget, J.; Valeur, B. *J. Photochem.* **1987**, *37*, 69.

10.1021/ic049256m CCC: $27.50
Published on Web 12/02/2004

interesting perspectives for the study of intramolecular metal to metal charge transfer as well as photoinduced geometrical changes.[5]

During the past few years, we have been interested in the construction of metallo-ligands based on organometallic systems and their possible application in the synthesis of homo-/hetero-binuclear complexes.[6] In this direction reactivity of CPI with the (arene)ruthenium complexes [{(η^6-arene)-Ru(μ-Cl)Cl}$_2$] was examined under varying reaction conditions. In this paper we report the synthetic aspects of a series of neutral mononuclear complexes [(η^6-arene)RuCl$_2$(CPI)] which could behave as metallo-ligands, their spectral properties and reactivity, and molecular structures of [(η^6-$C_{10}H_{14}$)-RuCl$_2$(CPI)] (**2**), [(η^6-C_6Me_6)RuCl$_2$(CPI)] (**3**), [(η^6-C_6H_6)-RuCl(CPI)(PPh_3)]PF_6·CH_2Cl_2 (**1a**), and [(η^6-$C_{10}H_{14}$)RuCl-(CPI)(PPh_3)]BF_4 (**2a**), along with interaction studies.

Experimental Section

Materials. All the synthetic manipulations were performed under oxygen-free nitrogen atmosphere. The solvents were dried and distilled before use by following the standard procedures. α-Phellandrene (Fluka), triphenylphosphine, triphenylarsine, triphenylstibine, 2,2′-bipyridine, 1,10-phenanthroline, hydrated ruthenium(III) chloride, hexamethylbenzene, ammonium tetrafluoroborate, and ammonium hexafluorophosphate (all Aldrich) were used as received. The ligand 1-(4-cyanophenyl)imidazole and the precursor complexes [{(η^6-arene)Ru(μ-Cl)Cl}$_2$] were prepared and purified by following the literature procedures.[5,7−9]

Instrumentation. Elemental analyses of the complexes were performed at Sophisticated Analytical Instrument Facility, Central Drug Research Institute, Lucknow, India. Infrared spectra were recorded on a Perkin-Elmer-577 spectrophotometer. NMR spectra were obtained on Bruker-DRX300 MHz spectrometer with tetramethylsilane as an internal standard. Electronic and emission spectra of the complexes were obtained on a Shimadzu UV-1601 and Perkin-Elmer-LS 55 luminescence spectrometer, respectively. The FAB mass spectra were recorded on a JEOL SX 102/DA 6000 mass spectrometer using xenon (6 kV, 10 mA) as the FAB gas. The accelerating voltage was 10 kV, and the spectra were recorded at room temperature with *m*-nitrobenzyl alcohol as the matrix. Electrochemical data were acquired on a PAR model 273A electrochemistry system at a scan rate of 50 mV s^{-1}. The sample solutions (10^{-4} M) were prepared in purified acetonitrile containing $NEt_4^+ClO_4^-$ (0.1 M) as a supporting electrolyte. Solution was deoxygenated by bubbling nitrogen for about 20 min in each experiment. Platinum wire working and auxiliary electrodes and an aqueous saturated calomel reference electrode were used in a three-electrode configuration. **Caution!** *Care must be taken while working with perchlorate salts.*

Synthesis and Characterization. The complexes **1**−**3** were prepared by following the general procedure as described below for the complex **1**:

Synthesis of [(η^6-C_6H_6)RuCl$_2$(CPI)] (1). A suspension of [{(η^6-C_6H_6)Ru(μ-Cl)Cl}$_2$] (0.502 g, 1.0 mmol) in 25 mL of dichloromethane was treated with CPI (0.338 g, 2.0 mmol) and stirred at room temperature for 4 h. Slowly the suspension dissolved, and a bright yellow solution was obtained. The resulting solution was evaporated to dryness under reduced pressure, and the solid mass thus obtained was extracted with dichloromethane. It was filtered through Celite to remove any solid impurities, and light petroleum ether was added to the filtrate with stirring until it became turbid. A yellow-orange microcrystalline product separated which was separated by filtration, washed several times with petroleum ether (40−60 °C), and dried under vacuo. Yield: 0.334 g, 80%. Anal. Calcd for $C_{16}Cl_2H_{13}N_3Ru$: C, 45.82; H, 3.10; N, 10.02. Found: C, 45.78; H, 3.08; N, 10.00. IR (Nujol): 2226 cm^{-1} ν(C≡N). ^{1}H ($CDCl_3$): δ 5.94 (s, η^6-C_6H_6), 7.45 (d, 1H, 7.4 Hz), 7.76 (d, 1H, 6 Hz), 7.83 (d, 2H, 9 Hz), 8.02 (d, 2H, 9 Hz), 8.51 (s, 1H) ppm. ^{13}C ($CDCl_3$): δ 81.51 (C_6H_6), 111.14 (CN), 117.01, 120, 118, 131, 133, 138, 140.

Synthesis of [(η^6-$C_{10}H_{14}$)RuCl$_2$(CPI)] (2). This complex was prepared by treatment of [{(η^6-$C_{10}H_{14}$)Ru(μ-Cl)Cl}$_2$] (0.612 g, 1.0 mmol) with CPI (0.338 g, 2.0 mmol) in dichloromethane (25 mL) following the above procedure. It was separated as yellow-orange crystals. Yield: 0.403 g, 85%. Anal. Calcd for $C_{20}Cl_2H_{21}N_3Ru$: C, 50.52; H, 4.42; N, 8.84. Found: C, 50.58; H, 4.52; N, 8.86. IR (Nujol): 2225 cm^{-1} ν(C≡N). ^{1}H ($CDCl_3$): δ 1.30 (d, $CH(CH_3)_2$, 6.9 Hz), 2.22 (s, C−CH_3), 3.07 (sp, $CH(CH_3)_2$, 6.8 Hz), 5.30−5.50 (dd, C_6H_4, 6 Hz), 7.34 (d, 2H,6.0 Hz), 7.43 (d, 1H, 8.7 Hz), 7.48 (d, 2H, 6.0 Hz), 7.75 (d, 1H, 8.4 Hz), 8.38 (s, 1H). ^{13}C ($CDCl_3$): δ 22.2 ($CHMe_2$), 30.6 ($CHMe_2$), 81.4 (C_6H_4), 81.5 (C_6H_4), 97.5 (C−CH_3), 102.8 (C.$CHMe_2$), 111.8 (CN), 117.6, 118.3, 121, 133.8, 134.1, 138.1, 138.8. FAB$^+$, *m*/*z*: 440 ([M]$^+$), 271 ([M − CPI]$^+$), 235 ([M − CPI − Cl]$^+$).

Synthesis of [(η^6-C_6Me_6)RuCl$_2$(CPI)] (3). This was prepared by reacting [{(η^6-C_6Me_6)Ru(μ-Cl)Cl}$_2$] (0.668 g, 1.0 mmol) with CPI (0.338 g, 2.0 mmol) in 25 mL of dichloromethane. The yellow microcrystalline complex was filtered off and washed several times with petroleum ether and dried under vacuo. Yield: 0.428 g, 85%. Anal. Calcd for $C_{22}Cl_2H_{25}N_3Ru$: C, 52.49; H, 4.97; N, 8.35. Found: C, 52.34; H, 4.86; N, 8.28. IR (Nujol): 2222 cm^{-1} ν(C≡N). ^{1}H ($CDCl_3$): δ 2.07 (η^6-C_6Me_6), 7.44 (d, 2H, 9.0 Hz), 7.73 (d, 2H, 9.0 Hz), 7.83 (d, 1H, 3 Hz), 8.14 (d, 1H, 8.7 Hz), 8.29 (s, 1H). ^{13}C ($CDCl_3$): δ 15.40 (C_6Me_6), 93.18 (C_6Me_6), 111.5 (CN), 117.64, 121.29, 132.58, 133.93, 133.03, 137, 139.54.

The complexes **1a**−**e**, **2a**−**e**, and **3a**−**e** were prepared by following the general method described below for complex **1a**:

Synthesis of [(η^6-C_6H_6)RuCl(CPI)(PPh_3)]PF_6.CH_2Cl_2 (1a). To a suspension of complex **1**, [(η^6-C_6H_6)RuCl$_2$(CPI)] (0.419 g, 1.0 mmol), in 25 mL of methanol was added PPh_3 (0.262 g, 1.0 mmol), and contents of the flask were heated under reflux for 1 h. The resulting pale yellow solution was cooled to room temperature and filtered through Celite. Ammonium hexafluorophosphate dissolved in 10 mL of methanol was added to the filtrate. Just after addition of salt, a yellow crystalline solid separated. It was filtered out and washed several times with methanol and diethyl ether. Yield: 0.718 g, 82%. Anal. Calcd for $C_{35}Cl_3F_6H_{30}N_3P_2Ru$: C, 47.94; H, 3.42; N, 4.79. Found: C, 47.88; H, 3.44; N, 4.68. IR (Nujol): 2227 cm^{-1} ν(C≡N). ^{1}H ($CDCl_3$): δ 5.97 (η^6-C_6H_6), 7.30−7.45 (br m, aromatic protons of PPh_3), 7.99 (d, 1H, 6 Hz), 7.83 (d, 2H, 9.0 Hz), 7.72 (d, 2H, 9.0 Hz), 8.42 (s, 1H), 7.75 (d, 1H, 6 Hz), 6.85 (d, 1H, 6.7 Hz).

(4) Schenter, G. K.; Duke, C. B. *Chem. Phys. Lett.* **1991**, *176*, 563.
(5) Hatzidimitriou, A.; Gourdon, A.; Devillers, J.; Launay, J.-P.; Mena, E.; Amouyal, E. *Inorg. Chem.* **1996**, *35*, 2212.
(6) (a) Gupta, D. K.; Sahay, A. N.; Pandey, D. S.; Jha, N. K.; Sharma, P.; Espinosa, G.; Cabrera, A.; Puerta, M. C.; Valerga, P. *J. Organomet. Chem.* **1998**, *568*, 13. (b) Sahay, A. N.; Pandey, D. S.; Walwalkar, M. G. *J. Organomet. Chem.* **2000**, *605*, 74. (c) Singh, A.; Singh, N.; Pandey, D. S. *J. Organomet. Chem.* **2002**, *642*, 48.
(7) Robertson, D. R.; Robertson, I. W.; Stephenson, T. A. *J. Organomet. Chem.* **1980**, *202*, 309.
(8) Bennett, M. A.; Smith, A. K. *J. Chem. Soc., Dalton Trans.* **1974**, 233.
(9) Bennett, M. A.; Huang, T. N.; Matheson, T. W.; Smith, A. K. *Inorg. Synth.* **1982**, *21*, 74.

^{31}P (dmso-D_6): δ 36.57 (s). FAB$^+$, *m*/*z*: 646 ([M]$^+$), 477 ([M − CPI]$^+$), 441 ([M − CPI − Cl]$^+$).

Characterization Data for [(η^6-$C_{10}H_{14}$)RuCl(CPI)(PPh_3)]BF_4 (2a). Orange crystals were formed. Yield: 0.577 g, 73%. Anal. Calcd for $BC_{38}ClF_4H_{36}N_3PRu$: C, 57.72; H, 4.56; N, 5.32. Found: C, 57.78; H, 4.78; N, 5.49. IR (Nujol): 2228 cm^{-1} ν(C≡N). ^{1}H ($CDCl_3$): δ 1.30 (d, $CH(CH_3)_2$, 6.9 Hz), 2.22 (s, C−CH_3), 3.07 (sp, $CH(CH_3)_2$, 6.8 Hz), 5.30−5.50 (dd, C_6H_4, 6 Hz), 7.28−7.48 (br m, aromatic protons of PPh_3), 7.81 (s, 1H), 7.63 (d, 1H, 8.4 Hz), 8.06 (d, 1H, 8.1 Hz), 8.42 (s, 1H). ^{31}P (dmso-D_6): 36.56 (s). FAB$^+$, *m*/*z*: 703 ([M]$^+$), 534 ([M − CPI]$^+$), 498 ([M − CPI − Cl]$^+$).

Characterization Data for [(η^6-C_6Me_6)RuCl(CPI)(PPh_3)]PF_6 (3a). Greenish crystals were formed. Yield: 0.631 g, 72%. Anal. Calcd for $C_{40}ClF_6H_{40}N_3P_2Ru$: C, 54.79; H, 4.56; N, 4.79. Found: C, 54.92; H, 4.89; N, 4.92. IR (Nujol): 2230 cm^{-1} ν(C≡N). ^{1}H ($CDCl_3$): δ 1.83 (η^6-C_6Me_6), 7.21−7.57 (br m, aromatic protons of PPh_3), 7.76 (d, 2H, 7.5 Hz), 7.57 (d, 2H, 8.1 Hz), 7.32 (d, 1H, 8.4 Hz), 7.24 (d, 1H, 6.0 Hz), 8.39 (s, 1H). ^{31}P (dmso-D_6): 35.98 (s). FAB$^+$, *m*/*z*: 731 ([M]$^+$), 562 ([M − CPI]$^+$), 526 ([M − CPI − Cl]$^+$).

Characterization Data for [(η^6-C_6H_6)RuCl(CPI)($AsPh_3$)]PF_6 (1b). Red crystals were formed. Yield: 0.662 g, 79%. Anal. Calcd for $AsC_{34}ClF_6H_{28}N_3PRu$: C, 48.69; H, 3.34; N, 5.01. Found: C, 48.94; H, 3.37; N, 5.12. IR (Nujol): 2227 cm^{-1} ν(C≡N). ^{1}H ($CDCl_3$): δ 5.94 (η^6-C_6H_6), 7.25−7.61 (br m, aromatic protons of $AsPh_3$), 7.45 (s, 1H), 7.76 (s, 1H), 7.83 (d, 1H, 8.7 Hz), 8.02 (d, 1H, 5.9 Hz), 8.51 (s, 1H).

Characterization Data for [(η^6-$C_{10}H_{14}$)RuCl(CPI)($AsPh_3$)]BF_4 (2b). Yellow crystals were formed. Yield: 0.571 g, 68.5%. Anal. Calcd for $AsBC_{38}ClF_4H_{36}N_3Ru$: C, 54.74; H, 4.32; N, 5.04. Found: C, 54.68; H, 4.41; N, 5.06. IR (Nujol): 2230 cm^{-1} ν(C≡N). ^{1}H ($CDCl_3$): δ 1.30 (d, $CH(CH_3)_2$, 6.9 Hz), 2.22 (s, C−CH_3), 3.07 (sp, $CH(CH_3)_2$, 6.8 Hz), 5.30−5.50 (dd,C_6H_4, 6 Hz), 7.27−7.58 (br m, aromatic protons of $AsPh_3$), 7.43 (d, 1H, 6.5 Hz), 7.80 (d, 1H,6.3 Hz), 7.86 (d, 2H, 9.1 Hz), 8.09 (d, 2H, 5.8 Hz), 8.63 (s, 1H). FAB$^+$, *m*/*z*: 746 ([M]$^+$), 577 ([M − CPI]$^+$), 541 ([M − CPI − Cl]$^+$).

Characterization Data for [(η^6-C_6Me_6)RuCl(CPI)($AsPh_3$)]BF_4 (3b). Orange crystals were formed. Yield: 0.577 g, 67%. Anal. Calcd for $AsBC_{40}ClF_4H_{40}N_3Ru$: C, 55.75; H, 4.65; N, 4.88. Found: C, 55.91; H, 4.84; N, 4.76. IR (Nujol): 2229 cm^{-1} ν(C≡N). ^{1}H ($CDCl_3$): δ 1.82 (η^6-C_6Me_6), 7.03−7.23 (br m, aromatic protons of $AsPh_3$), 7.50 (d, 1H, 5.6 Hz), 7.79 (d, 1H, 5.1 Hz), 7.86 (d, 2H, 8.9 Hz), 8.13 (d, 2H, 6.1 Hz), 8.59 (s, 1H). FAB$^+$, *m*/*z*: 774 ([M]$^+$), 605 ([M − CPI]$^+$), 569 ([M − CPI − Cl]$^+$).

Characterization Data for [(η^6-C_6H_6)RuCl(CPI)($SbPh_3$)]PF_6 (1c). Dark red crystals were formed. Yield: 0.715 g, 81%. Anal. Calcd for $C_{34}ClF_6H_{28}N_3PruSb$: C, 46.21; H, 3.17; N, 4.76. Found: C, 46.28; H, 3.27; N, 4.72. IR (Nujol): 2228 cm^{-1} ν(C≡N). ^{1}H ($CDCl_3$): δ 6.03 (η^6-C_6H_6), 7.20−7.43 (br m, aromatic protons of $SbPh_3$), 7.55 (d, 1H, 6.9 Hz), 7.79 (d, 1H, 7.3 Hz), 7.79 (d, 2H, 8.8 Hz), 7.98 (d, 2H, 5.9 Hz), 8.61 (s, 1H). FAB$^+$, *m*/*z*: 738 ([M]$^+$), 569 ([M − CPI]$^+$).

Characterization Data for [(η^6-$C_{10}H_{14}$)RuCl(CPI)($SbPh_3$)]BF_4 (2c). Brown orange crystals were formed. Yield: 0.625 g, 71%. Anal. Calcd for $BC_{38}ClF_4H_{36}N_3RuSb$: C, 51.76; H, 4.09; N, 4.77. Found: C, 51.46; H, 4.18; N, 4.47. IR (Nujol): 2227 cm^{-1} ν(C≡N). ^{1}H ($CDCl_3$): δ 2.07 (η^6-$C_{10}H_{14}$), 7.14−7.35 (br m, aromatic protons of $SbPh_3$), 7.56 (d, 1H, 6.6 Hz), 7.83 (d, 1H, 6.2 Hz), 7.91 (d, 2H, 8.9 Hz), 8.07 (d, 2H, 6.3 Hz), 8.53 (s, 1H). FAB$^+$, *m*/*z*: 794 ([M]$^+$), 625 ([M − CPI]$^+$).

Characterization Data for [(η^6-C_6Me_6)RuCl(CPI)($SbPh_3$)]BF_4 (3c). An orange crystalline solid was formed. Yield: 0.668 g, 73.5%. Anal. Calcd for $BC_{40}ClF_4H_{40}N_3RuSb$: C, 52.81; H, 4.40; N, 4.62. Found: C, 52.59; H, 4.71; N, 4.68. IR (Nujol): 2231 cm^{-1} ν(C≡N). ^{1}H ($CDCl_3$): δ 2.03 (η^6-C_6Me_6), 7.26−7.45 (br m, aromatic protons of $SbPh_3$), 7.36 (d, 1H, 6.2 Hz), 7.81 (d, 1H, 4.9 Hz), 7.87 (d, 2H, 8.9 Hz), 8.10 (d, 2H, 6.1 Hz), 8.49 (s, 1H). FAB$^+$, *m*/*z*: 822 ([M]$^+$), 653 ([M − CPI]$^+$).

Characterization Data for [(η^6-C_6H_6)Ru(bipy)(CPI)][PF_6]$_2$ (1d). Dark red crystals were formed. Yield: 0.572 g, 72%. Anal. Calcd for $C_{26}F_{12}H_{21}N_5P_2Ru$: C, 39.29; H, 2.64; N, 8.82. Found: C, 39.41; H, 2.48; N, 8.45. IR (Nujol): 2230 cm^{-1} ν(C≡N). ^{1}H ($CDCl_3$): δ 9.77 (d, 2H, 5.4 Hz), 9.60 (d, 2H, 5.7 Hz), 8.79 (dt, 2H, 7.7 Hz), 8.88 (s, 1H), 8.62 (d, 1H, 4.8 Hz), 7.74 (m, 2H), 7.90 (d, 2H, 6.4 Hz), 7.84 (d, 2H, 6.4 Hz), 6.09 (s, 6H), 7.75 (d, 1H, 6.6 Hz). FAB$^+$, *m*/*z*: 504 ([M]$^+$), 336 ([M − CPI]$^+$).

Characterization Data for [(η^6-$C_{10}H_{14}$)Ru(bipy)(CPI)][PF_6]$_2$ (2d). Pale yellow crystals were formed. Yield: 0.586 g, 69%. Anal. Calcd for $C_{30}F_{12}H_{29}N_5P_2Ru$: C, 42.35; H, 3.41; N, 8.23. Found: C, 42.45; H, 3.55; N, 7.99. IR (Nujol): 2235 cm^{-1} ν(C≡N). ^{1}H ($CDCl_3$): δ 1.30 (d, $CH(CH_3)_2$, 6.9 Hz), 2.22 (s, C−CH_3), 3.07 (sp, $CH(CH_3)_2$, 6.8 Hz), 5.30−5.50 (dd, C_6H_4, 6 Hz), 9.67 (d, 2H, 5.6 Hz), 9.50 (d, 2H, 5.7 Hz), 8.69 (dt, 2H, 7.6 Hz), 8.78 (s, 1H), 8.52 (d, 1H, 4.9 Hz), 7.64 (m, 2H), 7.80 (d, 2H, 6.5 Hz), 7.74 (d, 2H, 6.6 Hz), 7.65 (d, 1H, 6.6 Hz). FAB$^+$, *m*/*z*: 560 ([M]$^+$), 391 ([M − CPI]$^+$).

Characterization Data for [(η^6-C_6Me_6)Ru(bipy)(CPI)][BF_4]$_2$ (3d). Yellow crystals were formed. Yield: 0.564 g, 74%. Anal. Calcd for $B_2C_{32}F_8H_{33}N_5Ru$: C, 50.39; H, 4.33; N, 9.19. Found: C, 50.66; H, 4.39; N, 8.96. IR (Nujol): 2234 cm^{-1} ν(C≡N). ^{1}H ($CDCl_3$): δ 2.03 (η^6-C_6Me_6), 9.57 (d, 5.5 Hz, 2H), 9.40 (d, 2H, 5.6 Hz), 8.59 (dt, 2H, 7.8 Hz), 8.68 (s, 1H), 8.42 (d, 1H, 4.8 Hz), 7.54 (m, 2H), 7.70 (d, 2H, 6.4 Hz), 7.64 (d, 2H, 6.7 Hz), 7.75 (d, 1H, 6.6 Hz). FAB$^+$, *m*/*z*: 588 ([M]$^+$), 419 ([M − CPI]$^+$).

Characterization Data for [(η^6-C_6H_6)Ru(phen)(CPI)][PF_6]$_2$ (1e). Brown crystals were formed. Yield: 0.499 g, 61%. Anal. Calcd for $C_{28}F_{12}H_{21}N_5P_2Ru$: C, 41.08; H, 2.57; N, 8.56. Found: C, 41.22; H, 2.68; N, 8.39. IR (Nujol): 2233 cm^{-1} ν(C≡N). ^{1}H ($CDCl_3$): δ 9.48 (d, 2H, 5.3 Hz), 8.80 (d, 2H, 8.4 Hz), 8.28 (s, 2H), 8.10 (dd, 2H, 8.4 Hz), 9.83 (s, 1H), 7.42 (s, 6H, C_6H_6), 7.85 (d, 2H, 6 Hz), 7.79 (d, 2H, 9 Hz), 7.59 (d, 1H, 6 Hz), 7.41 (d, 1H, 6 Hz). FAB$^+$, *m*/*z*: 528 ([M]$^+$), 359 ([M − CPI]$^+$).

Characterization Data for [(η^6-$C_{10}H_{14}$)Ru(phen)CPI][PF_6]$_2$ (2e). Yellow crystals were formed. Yield: 0.655 g, 75%. Anal. Calcd for $C_{32}H_{29}F_{12}N_5P_2Ru$: C, 43.93; H, 3.32; N, 8.01. Found: C, 43.70; H, 3.08; N, 8.12. IR (Nujol): 2232 cm^{-1} ν(C≡N). ^{1}H ($CDCl_3$): δ 1.30 (d, $CH(CH_3)_2$, 6.9 Hz), 2.22 (s, C−CH_3), 3.07 (sp, $CH(CH_3)_2$, 6.8 Hz), 5.30−5.50 (dd, C_6H_4, 6 Hz), 9.28 (d, 2H, 5.3 Hz), 8.60 (d, 2H, 8.4 Hz), 8.08 (s, 2H), 8.00 (dd, 2H, 8.4 Hz), 9.63 (s, 1H), 7.22 (s, 6H), 7.65 (d, 2H, 6 Hz), 7.59 (d, 2H, 9 Hz), 7.39 (d, 1H, 6 Hz), 7.21 (d, 1H, 6 Hz). FAB$^+$, *m*/*z*: 584 ([M]$^+$), 415 ([M − CPI]$^+$).

Characterization Data for [(η^6-C_6Me_6)Ru(phen)CPI][BF_4]$_2$ (3e). Pale yellow crystals were formed. Yield: 0.558 g, 71%. Anal. Calcd for $B_2C_{34}F_8H_{33}N_5Ru$: C, 51.91; H, 4.20; N, 8.91. Found: C, 51.65; H, 4.30; N, 9.02. IR (Nujol): 2229 cm^{-1} ν(C≡N). ^{1}H ($CDCl_3$): δ 2.03 (η^6-C_6Me_6), 9.38 (d, 2H, 5.3 Hz), 8.70 (d, 2H, 8.4 Hz), 8.18 (s, 2H), 8.10 (dd, 2H, 8.4 Hz), 9.73 (s, 1H), 7.32 (s, 6H), 7.75 (d, 2H, 6 Hz), 7.69 (d, 2H, 9 Hz), 7.49 (d, 1H, 6 Hz), 7.31 (d, 1H, 6 Hz). FAB$^+$, *m*/*z*: 612 ([M]$^+$), 419 ([M − CPI]$^+$).

Characterization Data for [(η^6-$C_{10}H_{14}$)$RuCl_2$(μ-CPI)Ru(η^6-C_6H_6)Cl_2] (2f). A solution of the complex **2**, [(η^6-$C_{10}H_{14}$)$RuCl_2$-(CPI)] (0.475 g, 1 mmol), in 25 mL of dichloromethane was treated

with dimeric complex [(η^6-C_6H_6)Ru(μ-Cl)Cl}$_2$] (0.502 g, 1 mmol), and the resulting solution was stirred at room temperature for about 6 h. Slowly it turned brown, and a clear solution was obtained. It was filtered and concentrated under reduced pressure. The solid mass thus obtained was extracted with dichloromethane and filtered, and the filtrate was layered with light petroleum ether and left for slow crystallization. After a couple of days a brown microcrystalline product was obtained. It was filtered out, washed several times with petroleum ether, and dried under vacuo. Yield: 0.500 g, 69%. Anal. Calcd for $C_{26}Cl_4H_{27}N_3Ru_2$: C, 43.03; H, 3.72; N, 5.79. Found: C, 42.98; H, 3.70; N, 5.81. IR (Nujol): 2208 cm^{-1} ν(C≡N). ^{1}H ($CDCl_3$): δ 1.30 (d, $CH(CH_3)_2$, 6.9 Hz) 2.22 (s, C−CH_3), 3.07 (sp, $CH(CH_3)_2$, 6.8 Hz), 5.30−5.50 (dd, C_6H_4, 6 Hz), 7.42 (s, 6H, C_6H_6), 7.34 (d, 1H, 6.7 Hz), 7.43 (d, 2H, 8.7 Hz), 7.48 (d, 1H, 8.4 Hz), 7.75 (d, 2H, 8.4 Hz), 8.38 (s, 1H).

Characterization Data for [(η^6-$C_{10}H_{14}$)$RuCl_2$(μ-CPI)Ru(η^6-C_6Me_6)Cl_2] (2g). A red brown compound formed. Yield: 0.566 g, 70%. Anal. Calcd for $C_{32}Cl_4H_{39}N_3Ru_2$: C, 47.47; H, 4.82; N, 5.19. Found: C, 47.58; H, 4.80; N, 5.16. IR (Nujol): 2212 cm^{-1} ν(C≡N). ^{1}H ($CDCl_3$): δ 1.26 (d, $CH(CH_3)_2$, 6.9 Hz), 2.31 (s, C−CH_3), 3.10 (sp, $CH(CH_3)_2$, 6.9 Hz), 5.29−5.52 (dd, C_6H_4, 6.1 Hz), 2.06 (η^6-C_6Me_6), 7.35 (d, 1H, 5.9 Hz), 7.47 (d, 2H, 8.8 Hz), 7.49 (d, 1H, 8.3 Hz), 7.71 (d, 2H, 8.3 Hz), 8.41 (s, 1H).

X-ray Structure Determinations. Crystals suitable for single-crystal X-ray analyses for the complex [(η^6-$C_{10}H_{14}$)Ru(CPI)Cl_2] (**2**), [(η^6-C_6Me_6)Ru(CPI)Cl_2] (**3**), [(η^6-C_6H_6)RuCl(CPI)(PPh_3)]PF_6·CH_2Cl_2 (**1a**), and [(η^6-$C_{10}H_{14}$)RuCl(CPI)(PPh_3)]BF_4 (**2a**) were grown from CH_2Cl_2/petroleum ether (40−60 °C) at room temperature. Preliminary data on the space group and unit cell dimensions as well as intensity data were collected on Enraf-Nonius MACH3 diffractometer using graphite-monochromatized Mo Kα radiation. The crystal orientation, cell refinement, and intensity measurements were made using the program CAD-4 PC. The structure was solved by direct methods and refined by using MAXUS (1999) and SHELX-97.[10] The non-hydrogen atoms were refined with anisotropic thermal parameters. All the hydrogen atoms were geometrically fixed and allowed to refine using a riding model. The computer program PLATON was used for analyzing the interaction and stacking distances.[10]

Results and Discussion

Synthesis and Characterization of the Complexes. The new series of piano-stool complexes [(η^6-arene)$RuCl_2$(CPI)] was obtained in excellent yield in the usual manner by reacting the chloro-bridged dimers [{(η^6-arene)Ru(μ-Cl)Cl}$_2$] with an excess of CPI in dichloromethane at room temperature (Scheme 1).

Complexes **1**−**3** are air-stable solids and soluble in water and other common organic solvents and do not show any signs of decomposition in solution upon exposure to air for days. It was observed that in the reactions involving formation of the complexes **1**−**3** no intermediates were isolated, it is supposed that the reactions pass through chloro bridge cleavage and coordination of the CPI through imidazole nitrogen.

Scheme 1

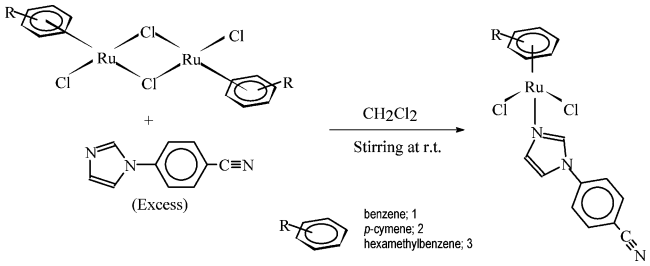

The complexes **1**−**3** reacted with EPh_3 (E = P, As or Sb) and N−N donor bases such as 2,2′-bipyridine and 1,10-phenanthroline afforded new cationic complexes [(η^6-arene)RuCl(CPI)(EPh_3)]$^+$ (η^6-arene = C_6H_6, E = P (**1a**), E = As (**1b**), E = Sb (**1c**); η^6-arene = $C_{10}H_{14}$, E = P (**2a**), E = As (**2b**), E = Sb (**2c**); η^6-arene = C_6Me_6, E = P (**3a**), E = As (**3b**), E = Sb (**3c**)) and [(η^6-arene)Ru(N−N)(CPI)]$^+$ (η^6-arene = C_6H_6, N−N = bipy (**1d**), N−N = phen (**1e**); η^6-arene = $C_{10}H_{14}$, N−N = bipy (**2d**), N−N = phen (**2e**); η^6-arene = C_6Me_6, N−N = bipy (**3d**), N−N = phen (**3e**)), which were isolated as tetrafluoroborate or hexafluorophosphate salts (Scheme 2).

Instead of substitution of metal-bound CPI, a chloro group is being substituted in these reactions, suggesting that the metal to CPI bond in the complexes is quite strong which has further been supported by FAB-MS and structural data. This observation is contrary to our earlier findings on the closely related 4-cyanopyridine complexes [Ru(η^6-arene)Cl_2(CNPy)] (η^6-arene = benzene, *p*-cymene, and hexamethylbenzene; CNPy = 4-cyanopyridine) and η^3:η^3-bis(allyl) complex [Ru(η^3:η^3-$C_{10}H_{14}$)Cl_2(CNPy)] (η^3:η^3-$C_{10}H_{14}$ = 2,7-dimethyloctdienedienyl) wherein the metal-bound 4-cyanopyridine was displaced by the respective bases, but not the chloro ligand, leading to the formation of [Ru(η^6-arene)Cl_2(EPh_3)] and [Ru(η^3:η^3-$C_{10}H_{14}$)Cl_2(EPh_3)], respectively.[6] In the reactions involving N−N donor bases both chloro groups are displaced by the incoming ligand bipy or phen to form [(η^6-arene)Ru(CPI)(N−N)]$^{2+}$.

Furthermore, the complex **2** reacted with dimers [{(η^6-arene)Ru(μ-Cl)Cl}$_2$] (η^6-arene = benzene or hexamethylbenzene) to give binuclear complexes [(η^6-$C_{10}H_{14}$)Cl_2Ru(μ-CPI)Ru(η^6-C_6H_6)Cl_2] (**2f**) and [(η^6-$C_{10}H_{14}$)Cl_2Ru(μ-CPI)Ru(η^6-C_6Me_6)Cl_2] (**2g**), wherein the CPI acts as a bridge between two metal centers (Scheme 3).

Analytical data of the complexes conformed well to their respective formulations. Information about composition of the complexes was also obtained from ESMS and FAB-MS spectra of the complexes (recorded in the Experimental Section). The position of various peaks and overall fragmentation pattern in the FAB-MS spectra of respective complexes conformed well to respective formulations. More information about the structure and bonding in the complexes has been deduced from the spectral studies.

The IR spectra of mononuclear complexes **1**−**3** and cationic complexes **1a**−**e**, **2a**−**e**, and **3a**−**e** displayed sharp and intense bands around 2226 cm^{-1} corresponding to ν(C≡N). The position of the ν(C≡N) remained unaltered, compared to that in the ligand itself; this suggested linkage

(10) (a) Mackay, S.; Dong, W.; Edwards, C.; Henderson, A.; Gilmox, C.; Stewart, N.; Shankland, K.; Donald, A. University of Glasgow, Scotland, 1999. (b) Sheldrick, G. M. *SHELX-97: Programme for refinement of crystal structures*; University of Gottingen: Gottingen, Germany, 1997. (c) PLATON, Spek, A. L. *Acta Crystallogr.* **1990**, *A46*, C31.

Scheme 2

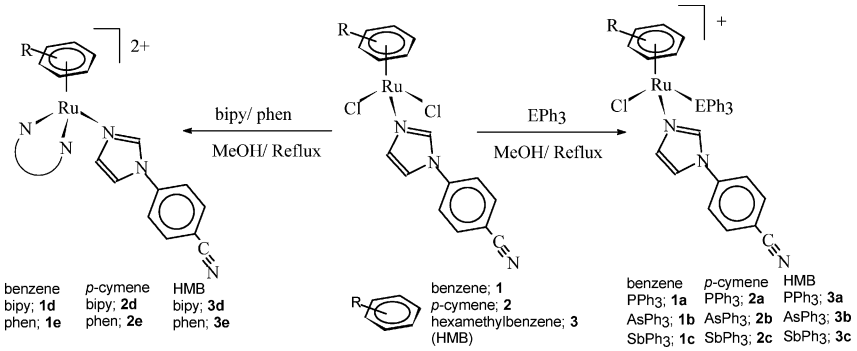

Scheme 3

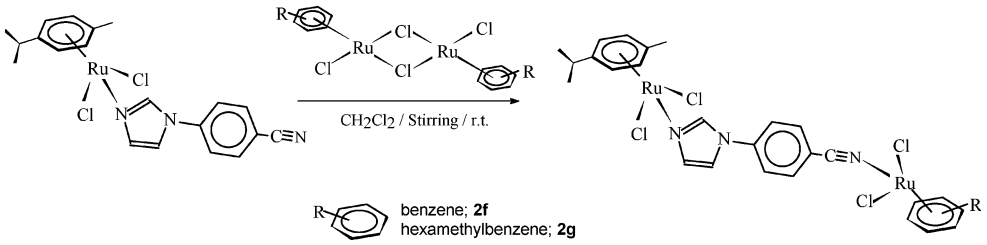

Table 1. Electronic and Emission Spectral Data for the Complexes

complexes	absorbance λ_{max}/nm (ϵ/M^{-1} cm^{-1})	emission λ_{max}/nm
$[(\eta^6\text{-}C_6H_6)RuCl_2(CPI)]$ (**1**)	400 (1008), 315 (20 246), 267 (31 292)	450
$[(\eta^6\text{-}C_6H_6)RuCl(CPI)(PPh_3)](PF_6)CH_2Cl_2$ (**1a**)	332 (4156), 264 (52 478)	408
$[(\eta^6\text{-}C_6H_6)RuCl(CPI)(AsPh_3)](PF_6)$ (**1b**)	328 (845), 260 (19 160)	443
$[(\eta^6\text{-}C_6H_6)RuCl(CPI)(SbPh_3)](PF_6)$ (**1c**)	386 (2396), 270 (72 246)	448
$[(\eta^6\text{-}C_6H_6)Ru(bipy)CPI](PF_6)_2$ (**1d**)	350 (20 218), 317 (31 042), 287 (52 256).	
$[(\eta^6\text{-}C_6H_6)Ru(phen)CPI](PF_6)_2$ (**1e**)	355 (21 234), 317 (36 454), 267 (79 998)	476
$[(\eta^6\text{-}C_{10}H_{14})RuCl_2(CPI)]$ (**2**)	407 (1730), 335 (2055), 249 (36 123)	462[a]
$[(\eta^6\text{-}C_{10}H_{14})RuCl(CPI)(PPh_3)](BF_4)$ (**2a**)	338 (2543), 254 (39 640)	434
$[(\eta^6\text{-}C_{10}H_{14})RuCl(CPI)(AsPh_3)](BF_4)$ (**2b**)	388 (2286), 324 (42 285), 263 (45 042)	417
$[(\eta^6\text{-}C_{10}H_{14})RuCl(CPI)(SbPh_3)](BF_4)$ (**2c**)	389 (2691), 338 (3277), 260 (45 751)	418
$[(\eta^6\text{-}C_{10}H_{14})Ru(bipy)CPI](PF_6)_2$ (**2d**)	348 (3181), 316 (15 612), 304 (14 594), 255 (34 388)	460
$[(\eta^6\text{-}C_{10}H_{14})Ru(phen)CPI](PF_6)_2$ (**2e**)	367 (2758), 322 (60 000), 275 (39 365)	437
$[(\eta^6\text{-}C_{10}H_{14})RuCl_2(\mu\text{-}CPI)Ru(\eta^6\text{-}C_6H_6)Cl_2]$ (**2f**)	391 (2363), 333 (2875), 268 (34 362)	422
$[(\eta^6\text{-}C_{10}H_{14})RuCl_2(\mu\text{-}CPI)Ru(\eta^6\text{-}C_6Me_6)Cl_2]$ (**2g**)	397 (3365), 333 (7822), 268 (36 243)	427
$[(\eta^6\text{-}C_6Me_6)RuCl_2(CPI)]$ (**3**)	412 (1536), 342 (22 567), 267 (31 123)	475
$[(\eta^6\text{-}C_6Me_6)RuCl(CPI)(PPh_3)](PF_6)$ (**3a**)	336 (54 285), 250 (71 428), 233 (82 000)	444
$[(\eta^6\text{-}C_6Me_6)RuCl(CPI)(AsPh_3)](BF_4)$ (**3b**)	398 (2102), 334 (37 428), 252 (42 766)	427
$[(\eta^6\text{-}C_6Me_6)RuCl(CPI)(SbPh_3)](BF_4)$ (**3c**)	381 (2385), 318 (40 325), 260 (42 041)	411
$[(\eta^6\text{-}C_6Me_6)Ru(bipy)CPI](BF_4)_2$ (**3d**)	404 (2589), 369 (3155), 291 (19 822)	466
$[(\eta^6\text{-}C_6Me_6)Ru(phen)CPI](BF_4)_2$ (**3e**)	356 (6258), 293 (21 387), 270 (50 010)	472

[a] $\Phi = 0.027$.

of CPI with the metal center in the respective complexes through imidazole nitrogen.[5] The binuclear complexes **2f**,**g** displayed a shift in the position of ν(C≡N) to ∼2210 cm^{-1}. The shift in the position of the ν(C≡N) in binuclear complexes relative to that in the free ligand or mononuclear complexes could be attributed to kinematic effects arising from coordination of pendant nitrile group with another ruthenium center.

NMR Spectroscopy. The ^{1}H NMR spectral data of the complexes along with their assignments are recorded in the Experimental Section. In the ^{1}H NMR spectra of the neutral mononuclear complex **1**−**3** arene protons displayed downfield shift as compared to that in the respective precursor complexes.[9] Downfield shift in the position of the arene protons might result from the change in electron density on the metal center due to linkage of CPI through its imidazole nitrogen. The conjugative and electron-withdrawing abilities of the −CN group pulls electron density away from the imidazole nucleus toward itself, leading to a decrease of electron density on the metal center which, in turn, may pull more electron density away from the η^6-arene, leading to deshielding of η^6-arene protons. The ^{1}H NMR spectra of the EPh_3 containing complexes **1a**−**c**, **2a**−**c**, and **3a**−**c** or those of N−N donor bases **1d,e**, **2d,e**, and **3d,e** displayed signals associated with CPI, EPh_3, and bipy or phen.[8] The position and integrated intensity of various resonance supported well the presence of ligand CPI and formulation of the respective complexes. The nitrile carbon of the CPI in the complexes resonated in the range 106.6−111.8 ppm, while the other carbons of CPI resonated in the range 117.6−144.2 ppm.[11]

Electronic Spectroscopy. UV/vis absorption and emission data for the complexes are listed in Table 1. The low-spin

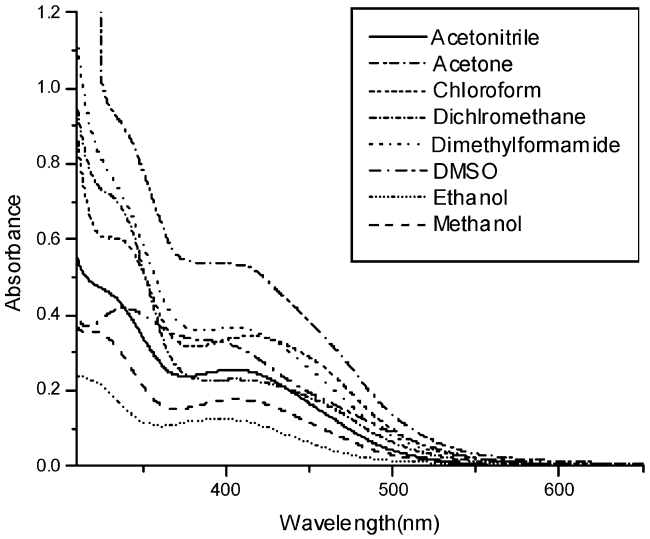

Figure 1. Electronic spectrum of the complex **2** in different solvents.

d^6 configuration of Ru(II) in the complexes [(η^6-arene)$RuCl_2$-(CPI)] provides filled t_{2g} orbital of proper symmetry for their interaction with relatively low-energy unoccupied π^* orbital of CPI. One therefore expects for a MLCT transition $t_{2g} \rightarrow \pi^*$ in these complexes, whose energy varies with the nature of the ligand acting as an acceptor. Electronic spectra of the mononuclear complexes showed moderately intense bands in the region 400−416, 350, and 290 nm (Table 1). The bands present in the range 400−416 nm have been assigned to MLCT transitions.[3,12] Further, it was observed that the position of λ_{max} in the electronic spectra of the complexes is sensitive to the nature of different solvents, showed positive solvatochromism, and is strong evidence in support of charge-transfer assignment (Figure 1). Since MLCT bands lead to separation of charge in the excited state, the transition energy of this band should be sensitive to the environment of the complex ion. The band in the region 350 nm also exhibited a small solvatochromic effect. This band has also been tentatively assigned to MLCT [Ru(II) $\rightarrow \pi^*$ arene]. The high-intensity absorption bands in the region 290 nm can be ascribed to the ligand-centered transition.[3,12a] Electronic spectra of the binuclear complexes **2f**,**g** displayed a significant blue shift (∼10 nm) in the position of λ_{max}. The shift in the position of λ_{max} could be attributed to asymmetrical nature of the bridging ligand. The π back-bonding from imidazole-bound ruthenium to the imidazole ring should raise the energy of π^* orbitals of the nitrile end, while the π back-bonding from the ruthenium to the NC group should also raise the energy of the imidazole π^* orbitals. Since energy of MLCT is related to that of LUMO of the ligand, increase in the energy of π^* by both the metal centers should result in a shift of MLCT bands toward higher frequency side with respect to that in the mononuclear complexes.[13]

Emission Spectroscopy. All the complexes are found to be luminescent at room temperature in dichloromethane. The relevant luminescence data for the complexes are listed in Table 1 (Figure 2). Complexes upon excitation in their respective lowest energy MLCT band maximum (340−410 nm) corresponding to the ruthenium−imidazole charge transfer resulted in a moderately strong emission (408−476 nm). The emission spectra are found to be parallel with their respective absorption bands so that these emission bands can be attributed to a metal to CPI MLCT band [Ru(dπ)−CPI-(π^*)], as the free CPI ligand does not emit at this wavelength.[5] The CPI molecule is planar in the ground state, due to the conjugation between imidazole and the benzonitrile. The HOMO is mainly located on the imidazole part whereas the LUMO is mainly localized on the phenyl ring containing the nitrile that results in intramolecular electron transfer.[5] The complexes **1**−**3** show much lower energy luminescence than their respective substitution products containing EPh_3 or N−N donor bases. This is consistent with the fact that the negatively charged ligands result in destabilization of the ground state and hence a decrease in the ^{3}MLCT-based luminescence. The presence of methyl substituents on the arene ring (benzene to hexamethylbenzene) shifts the emission band to lower energy side. This decrease in energy can be explained by an additional destabilization of the ground state (GS) with increasing effect of σ donor ligand.

Electrochemistry. A cyclic voltammogram of the representative complex [(η^6-C_6Me_6)$RuCl_2$(CPI)] (**3**) was obtained in CH_2Cl_2 containing 0.1 M TEAP at a sweep rate of 50 mV/s in the range −2.0 to +2.0 V as shown in Figure 3. It displayed a well-defined quasi-reversible oxidation reduction wave corresponding to a Ru(II)/Ru(III) redox couple with a half-wave potential $E_{1/2}$ of 1.152 V versus SCE and $E_{pa} - E_{pc} = 0.508$ V.[14] The waves associated with the Ru(II)/Ru-(III) redox couple in the complex **1** and **2** were observed at 1.32 and 1.18 V, respectively. One can see that as the methyl substitution at arene ligand increases from benzene to hexamethylbenzene, there is a shift in the position of Ru-(II)/Ru(III) redox couple toward less positive side. With an increase in methyl substitution on the coordinated arene ring, there is an increase in the electron density on the metal center. This results in a significant destabilization of the ground-state energy leading to a lowering of the metal-based oxidation potentials. As expected, there was not any wave due to the ligand CPI.[5]

Crystal Structures. Details about the data collection, solution, and refinement are presented in Table 2. Molecular structure of the complexes **2** and **3** and the complex cations of **1a** and **2a** with atomic numbering scheme is shown in Figure 4, and selected geometrical parameters and important bond parameters are presented in Table 3. Crystal packing in the complexes **2**, **3**, **1a**, and **2a** is stabilized by C−H···X type (X = Cl, F) inter- and intramolecular hydrogen bonding.

(11) Levy, G. C.; Nelson, G. L. *Carbon-13 Nuclear Magnetic Resonance*; Wiley-Interscience: New York, 1972; p 129.
(12) (a) Clarke, R. E.; Ford, P. C.; *Inorg. Chem.* **1970**, *9*, 227. (b) Curtis, J. C.; Sullivan, B. P.; Meyer, T. J. *Inorg. Chem.* **1983**, *22*, 224. (c) Didier, P.; Ortmans, I.; Kirschdemesmaeker, A.; Watts, R. J. *Inorg. Chem.* **1993**, *32*, 5239.
(13) (a) Sundberg, R. J.; Bryan, R. F.; Taylor; I. F.; Taube, H. *J. Am. Chem. Soc.* **1974**, *96*, 381. (b) Berger, R. M.; Ellis, D. D. *Inorg. Chim. Acta*. **1996**, *241*, 1.
(14) Sullivan, B. P.; Salmon, D. J.; Meyer, T. J. *Inorg. Chem.* **1978**, *17*, 5239.

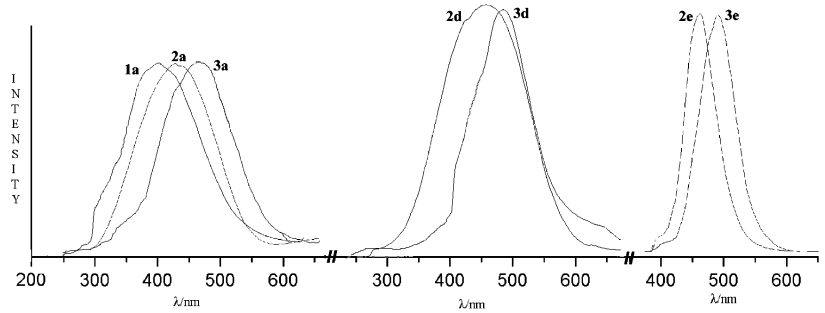

Figure 2. Normalized emission spectra of the complexes in CH_2Cl_2.

Table 2. Crystallographic Data for Complexes **2**, **3**, **1a**, and **2a**

	2	**3**	**1a**·CH_2Cl_2	**2a**
empirical formula	$C_{20}H_{21}Cl_2N_3Ru$	$C_{22}Cl_2H_{25}N_3Ru$	$C_{35}Cl_3H_{30}F_6N_3P_2Ru$	$C_{38}H_{36}BClF_4N_3PRu$
fw	475.37	503.42	875.98	789.00
cryst system	monoclinic	monoclinic	triclinic	monoclinic
space group	$P2_1$	$P2_1/c$	$P\bar{1}$	$P2_1/n$
a, Å	11.504(2)	12.2560(11)	11.1490(9)	12.6480(9)
b, Å	13.7250(8)	12.8320(13)	11.5520(12)	15.4830(8)
c, Å	13.2170(14)	14.3610(2)	15.0040(13)	18.5280(17)
α, deg	90.000(7)	90.00(10)	99.373(8)	90.000(6)
β, deg	105.232(13)	102.173(6)	97.987(7)	102.173(6)
γ, deg	90.000(10)	90.00(8)	106.853(8)	90.000(5)
V, Å^3	2013.6(5)	2189.9(4)	1788.9(3)	3546.7(5)
Z	4	4	2	4
d_{calc}, g cm^{-3}	1.568	1.527	1.626	1.478
μ, mm^{-1}	1.052	0.972	0.814	0.616
T, K	293(2)	293(2)	293(2)	293(2)
R_1 all	0.0299	0.0293	0.0597	0.0490
R_1 [$I > 2\sigma(I)$]	0.0270	0.0262	0.0463	0.0368
wR_2	0.0717	0.0723	0.1083	0.0977
wR_2 [$I > 2\sigma(I)$]	0.0689	0.0695	0.1168	0.0898

Table 3. Selected Bond Lengths (Å), Bond Angles (deg), and Torsion Angles (deg) in the Complexes

complex **2**		complex **3**		complex **1a**·CH_2Cl_2		complex **2a**	
Ru(1)−N(1)	2.097(12)	Ru−N(1)	2.124(2)	Ru−N(1)	2.124(4)	Ru(1)−N(1)	2.125(3)
Ru(1)−Cl(1)	2.427(4)	Ru−Cl(1)	2.4180(8)	Ru−Cl(1)	2.3971(13)	Ru(1)−Cl(1)	2.4007(10)
Ru(1)−Cl(2)	2.412(4)	Ru−Cl(2)	2.4236(7)	Ru−Ct	1.726	Ru(1)−Ct	1.719
Ru(1)−Ct	1.671	Ru−Ct	1.666	Ru−C_{av}	2.200	Ru(1)−C_{av}	2.224
Ru(1)−C_{av}	2.181	Ru−C_{av}	2.194	Ru−P(1)	2.3806(13)	Ru−P(1)	2.3715(11)
N(1)−C(11)	1.385(16)	N(1)−C(13)	1.319(3)	N(1)−C(25)	1.394(6)	N(1)−C(11)	1.323(4)
N(1)−C(12)	1.396(16)	N(1)−C(14)	1.381(4)	N(1)−C(27)	1.303(6)	N(1)−C(12)	1.378(5)
N(2)−C(11)	1.352(15)	N(2)−C(13)	1.355(3)	N(2)−C(26)	1.374(7)	N(2)−C(11)	1.347(5)
N(2)−C(13)	1.457(18)	N(2)−C(15)	1.380(4)	N(2)−C(27)	1.347(6)	N(2)−C(13)	1.366(5)
N(2)−C(14)	1.335(17)	N(2)−C(16)	1.429(3)	N(2)−C(28)	1.430(6)	N(2)−C(14)	1.438(5)
N(3)−C(20)	1.22(2)	N(3)−C(22)	1.126(4)	N(3)−C(34)	1.126(7)	N(3)−C(20)	1.132(6)
Cl(1)−Ru(1)−Cl(2)	88.79(14)	Cl(1)−Ru−Cl(2)	87.98(3)	N(1)−Ru−P(1)	89.14(10)	N(1)−Ru−P(1)	89.33(9)
Cl(1)−Ru(1)−N(1)	84.5(3)	Cl(1)−Ru−N(1)	86.53(6)	Cl(1)−Ru−N(1)	86.08(11)	N(1)−Ru−Cl(1)	86.22(8)
N(1)−Ru(1)−Cl(2)	86.7(3)	N(1)−Ru−Cl(2)	85.14(6)	P(1)−Ru−Cl(1)	86.05(4)	P(1)−Ru−Cl(1)	86.31(4)
C(13)−N(2)−C(14)−C(15)	−53.8(14)	C(13)−N(2)−C(16)−C(17)	42.4(4)	C(26)−N(2)−C(28)−C(32)	31.3(8)	C(13)−N(2)−C(14)−C(15)	−4.2(7)
C(11)−N(2)−C(14)−C(15)	31(2)	C(13)−N(2)−C(16)−C(21)	−37.1(3)	C(26)−N(2)−C(28)−C(29)	−149.0(6)	C(13)−N(2)−C(14)−C(19)	177.1(5)

Relevant bond distances and bond angles (please see Supporting Information) are corroborated well with the reported values.[15] Contact distances between C−H···F and C−H···Cl are 2.47−2.52 and 2.73−2.82 Å, respectively. These interactions may be called vdW interactions since the lengths are significantly less than the sum of van der Waals radii (2.8 and 3.1 Å, respectively). The C−H···Cl and C−H···N interaction in complex **2** leads to a rectangular grid network (Figure 5a). The crystal packing in the complex **3** also exhibits $\pi-\pi$ stacking interactions between hexamethylbenzene rings (arene−arene ring distance = 3.39 Å) (Figure 5b), and in complex **2a** it leads to a hexagonal network (Figure 5c).[15e]

The crystallographic asymmetric unit of the complex **2** contains two independent molecules, which are essentially identical. The metal center ruthenium in the complex **2** and **3** is coordinated through imidazole nitrogen N(1) from CPI, Cl(1), Cl(2), and arene ring in an η^6 manner. Similarly in complexes **1a** and **2a** ruthenium is coordinated by N(1) from CPI, the chloro group Cl(1), P(1) from PPh_3, and benzene

(15) (a) Braga, D.; Grepioni, F. *Chem. Commun.* **1996**, 571. (b) Steiner, T. *Angew. Chem., Int. Ed.* **2002**, *41*, 48. (c) Desiraju, G. R.; Steiner, T. *The weak hydrogen bond in structural chemistry and biology*; Oxford University Press: Oxford, U.K., 1999. (d) Braga, D.; Grepioni, F.; Tedesco, E. *Organometallics* **1998**, *17*, 2669. (e) Scaccianoce, L.; Braga, D.; Calhorda, M. J.; Grepioni, F.; Johnson, B. F. G. *Organometallics* **2000**, *19*, 790.

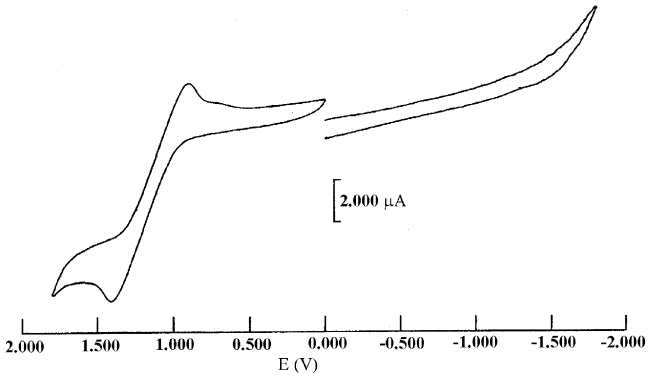

Figure 3. Cyclic voltammogram of the complex **3** in acetonitrile.

and *p*-cymene rings in an η^6-manner. Considering the arene rings as a single coordination site, overall coordination geometry about the metal center in the complexes **2, 3**, **1a**, and **2a** might be described as typical "piano-stool" geometry. The arene rings, *p*-cymene, hexamethylbenzene, or benzene ring in the respective complexes are almost planar, and ruthenium is displaced by 1.671, 1.666, 1.726, and 1.719 Å from centroid of the attendant arene ring in the complexes **2**, **3**, **1a**, and **2a**.[16] The Ru−Cl bond distances are normal and comparable with those observed in other Ru(II) arene complexes.[17] The Cl−Ru−Cl angles in the complexes **2** and **3** are comparable to those observed in other related systems.[18] The Ru to imidazole nitrogen distance are 2.097(12), 2.124-(2), 2.124(4), and 2.125(3) Å, respectively, in complex **2**, **3**, **1a**, and **2a** and followed a typical bonding pattern observed in other imidazole complexes.[19] These are comparable to Ru−N distances in closely related ligand 1-methyl-3-(4-cyanophenyl)imidazolium hexafluorophosphate and the Ru-(II) complexes [Ru(η^6-$C_{10}H_{14}$)Cl_2(CNPy)] and [Ru(η^3:η^3-$C_{10}H_{14}$)Cl_2(CNPy)].[5,6] The Ru−P distance in complex **1a** and **2a** are normal and comparable with Ru−P distances in other complexes.[20]

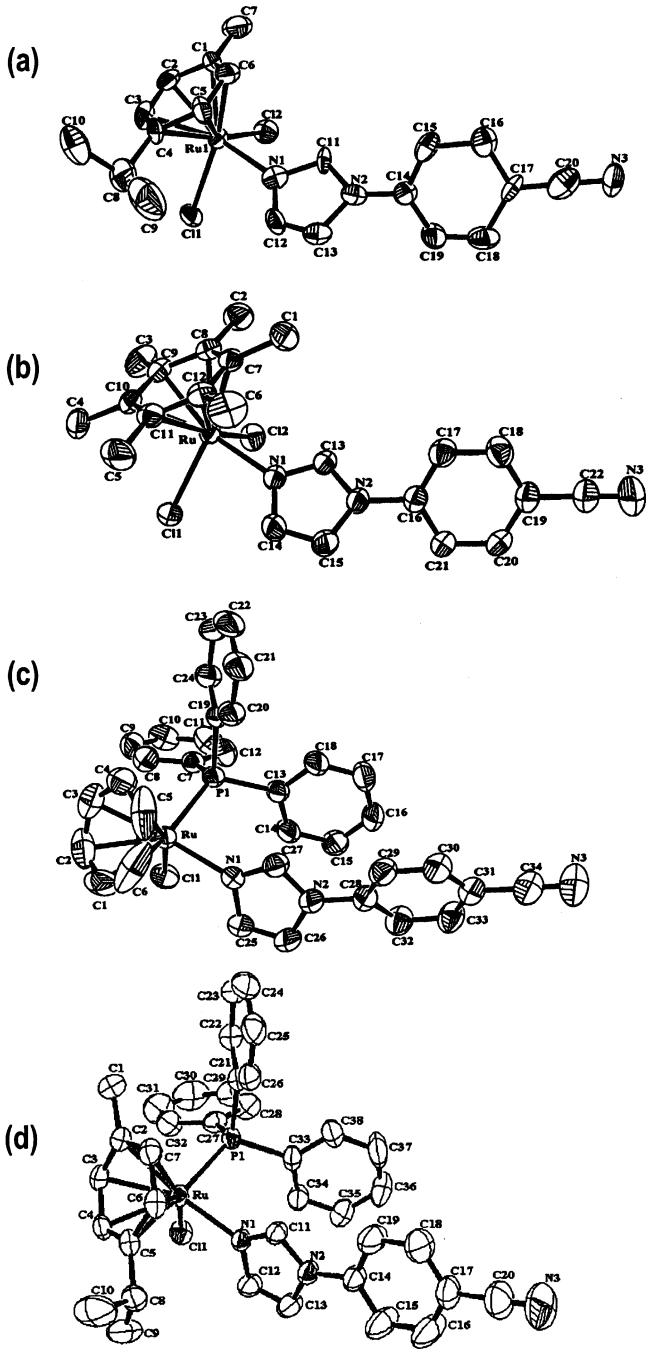

Figure 4. Molecular structures for (a) **2**, (b) **3**, (c) **1a**·CH_2Cl_2, and (d) **2a**.

In the complexes **2**, **3**, and **1a** the ligand CPI has lost planarity upon coordination with metal center. The cyanophenyl group of the ligand is not coplanar with imidazole ring and is tilted with respect to the imidazole ring plane at an angle of 31° (**2**), 42.4° (**3**), and 31.3° (**1a**) while in complex **2a** it is almost coplanar. The inter annular bond distance N(2)−C(14) is 1.335(17) Å in complex **2** which is

(16) (a) Campagna, S.; Denti, G.; Derosa, G.; Sabatino, L.; Ciano, M.; Balzani, V. *Inorg. Chem.* **1989**, *28*, 2565. (b) Schmehl, R. H.; Auerbach, R. A.; Wacholtz, W. F. *J. Phys. Chem.* **1988**, *92*, 6202. (c) Fuchs, Y.; Lofters, S.; Dieter, T.; Shi, W.; Morgan, R.; Strekas, T. C.; Gafney, H. D.; Baker, A. D. *J. Am. Chem. Soc.* **1987**, *109*, 2691. (d) Murphy, W. R.; Brewer, K. J.; Gettliffe, G.; Petersen, J. D. *Inorg. Chem.* **1989**, *28*, 81.

(17) (a) Watkins, S. F.; Fronczek, F. R. *Acta Crystallogr., Sect. B* **1982**, *38*, 270. (b) McCormick, F. B.; Cox, D. D.; Gleason, W. B. *Organometallics* **1993**, *12*, 610. (c) DiMarco, G.; Bartolotta, A.; Ricevuto, V.; Campagna, S.; Denti, G.; Sabatino, L.; Derosa, G. *Inorg. Chem.* **1991**, *30*, 270. (d) Luginbuhl, W.; Zbinden, P.; Pittet, P. A.; Armbruster, T.; Burgi, H.-B.; Merbach, A. E.; Ludi, A. *Inorg. Chem.* **1991**, *30*, 2350. (e) Davenport, A. J.; Davies, D. L.; Fawcett, J.; Garratt, S. A.; Russell, D. R. *J. Chem. Soc., Dalton Trans.* **2000**, 4432.

(18) (a) Bruce, M. I.; Wong, F. S.; Skelton, B. W.; White, A. H. *J. Chem. Soc., Dalton Trans.* **1981**, 1398. (b) Gould, R. O.; Jones, C. L.; Robertson, D. R.; Tocher, D. A.; Stephenson, T. A. *J. Organomet. Chem.* **1982**, *226*, 199. (c) Hayashida, T.; Nagashima, H. *Organometallics* **2002**, *21*, 3884. (d) Rath, R. K.; Nethaji, M.; Chakravarty, A. R. *J. Organomet. Chem.* **2001**, *633*, 79. (e) Nishiyama, H.; Konno, M.; Aoki, K. *Organometallics* **2002**, *21*, 2536. (f) Allardyce, C. S.; Dyson, P. J.; Ellis, D. J.; Heath, S. L. *Chem. Commun.* **2001**, 1396. (g) Frodl, A.; Herebian, D.; Sheldrick, W. S. *J. Chem. Soc., Dalton Trans.* **2002**, 3664. (h) Chen, H. M.; Parkinson, J. A.; Parsons, S.; Coxall, R. A.; Gould, R. O.; Sadler, P. J. *J. Am. Chem. Soc.* **2002**, *124*, 3064.

(19) (a) Bennett, M. A.; Robertson, G. B.; Smith, A. K. *J. Organomet. Chem.* **1972**, *43*, C41. (b) Elsegood, M. R. J.; Tocher, D. A. *Polyhedron* **1995**, *14*, 3147. (c) Menendez, C.; Morales, D.; Perez, J.; Riera, V.; Miguel, D. *Organometallics* **2001**, *20*, 2775.

(20) (a) Kratochvil, B.; Ondracek, J.; Velisek, J.; Hasek, J. *Acta Crystallogr., Sect.* C **1988**, *44*, 1579. (b) Alcalde, E.; Dinares, I.; Frigola, J.; Jaime, C.; Fayet, J.-P.; Vertut, M.-C.; Miravitlles, C.; Rius, J. *J. Org. Chem.* **1991**, *56*, 4223. (c) Johnson, C. R.; Jones, C. M.; Asher, S. A.; Abola, J. E. *Inorg. Chem.* **1991**, *30*, 2120.

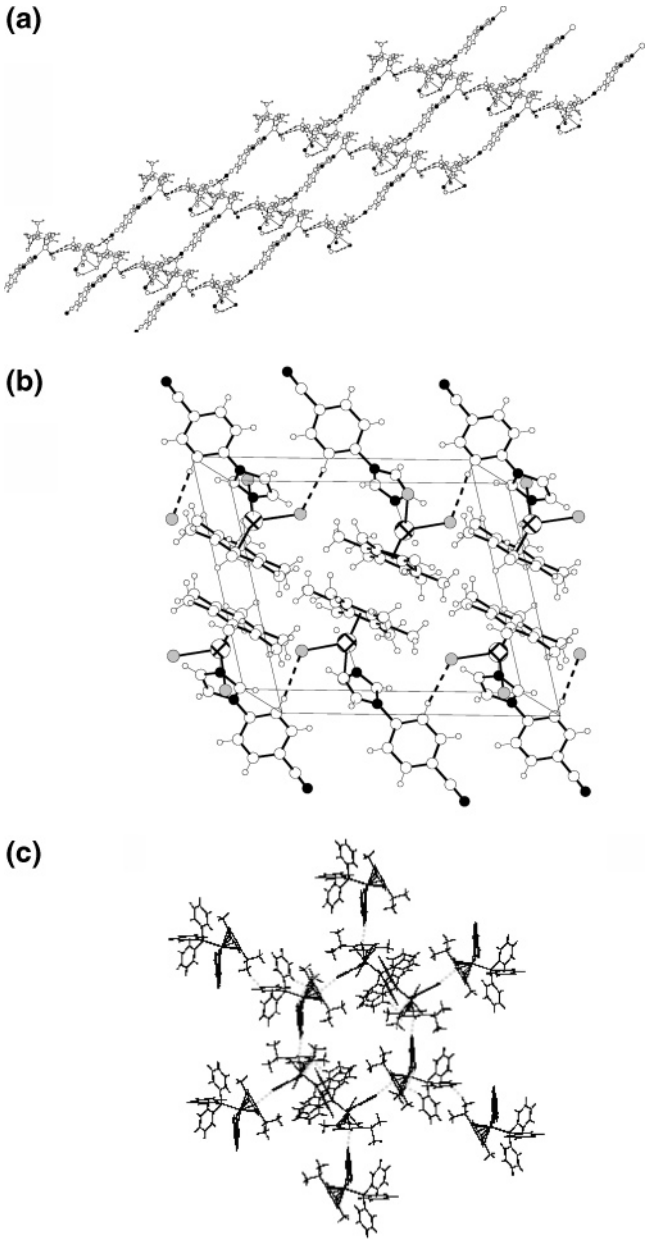

Figure 5. (a) Rectangular grid network in the crystal structure for complex **2**. (b) Crystal packing diagram for complex **3** showing the $\pi-\pi$ interaction. (c) Hexagonal planar network for complex **2a**.

slightly shorter than that in the complex **3** [N(2)−C(16) 1.429(3) Å], complex **1a** [N(2)−C(28) 1.430(6) Å], and complex **2a** [N(2)−C(14) 1.438(5) Å]. These are slightly shorter than a single C−N bond indicating a double-bond character. The nitrile C≡N bond lengths in the complexes **2**, **3**, **1a**, and **2a** are 1.22(2), 1.126(4), 1.126(7), and 1.132(6) Å, respectively. The C≡N bond distances in complexes **1a** and **2a** are comparable to each other, and these are shorter than that in the complex **2**. These are consistent with other reports.[5,6]

Conclusion. A series of new piano-stool complexes [Ru(η^6-arene)Cl_2(CPI)] (η^6-arene = benzene, *p*-cymene, and hexamethylbenzene), [(η^6-arene)RuCl(CPI)(EPh_3)]$^+$, and [(η^6-arene)Ru(N−N)(CPI)]$^{2+}$ incorporating the ligand CPI have been prepared, and linkage of CPI with the metal center through its imidazole nitrogen has been verified crystallographically. Further, the representative mononuclear complex [Ru(η^6-$C_{10}H_{14}$)Cl_2(CPI)] has been used as a metallo-ligand in the synthesis of homonuclear bimetallic complexes. Attempts to verify the molecular structure of the representative binuclear complex at our hands failed due to poor quality of the crystals. In the binuclear complexes two metal centers are bridged by a ligand exhibiting twisted internal charge transfer (TICT). The work toward development of homo-/hetero-binuclear mixed-valence binuclear complexes and study of their photophysical and photochemical properties is in progress in our laboratory.

Acknowledgment. Thanks are due to Department of Science and Technology, New Delhi, India, for financial assistance (SP/S1/F-04/2000). We also thank the Head, SAIF, Central Drug Research Institute, Lucknow, India, for providing analytical and spectral facilities. Special thanks are due to Prof. P. Mathur, Department of Chemistry, Indian Institute of Technology, Mumbai, India, and National Single Crystal X-ray Diffraction Facility, Indian Institute of Technology, Mumbai, India, for providing single-crystal X-ray data and Prof. T. K. Chandrasekhar, Department of Chemistry, Indian Institute of Technology, Kanpur, India, for providing emission spectral data.

Supporting Information Available: Crystallographic data for the complexes **2**, **3**, **1a**, and **2a** in CIF format and relevant bond distances, bond angles, and symmetries summarized in Table S1. This material is available free of charge via the Internet at http://pubs.acs.org.

IC049256M